

Use of pineapple peel biochar in the removal of Cu²⁺ ions in aqueous system: kinetics, isotherm and thermodynamics.

Marina Nunes dos Santos Silva^a, Giovanna Amaral Jorge Correia Guedes^a; Raissa Aguiar de Freitas^a, Beatriz Galdino Ribeiro^a, Marta Maria Menezes Bezerra Duarte^{a*}

^a Federal University of Pernambuco (UFPE), Department of Chemical Engineering, Av. dos Economistas, S/N, Recife, 50740-590, Brazil

Abstract

The disposal of industrial effluents containing copper (Cu²⁺) ions into water bodies can have a negative impact on human health and the environment, requiring removal prior to waste disposal. Among the techniques used to remove metals from effluents, the adsorption stands out due to its simplicity and possibility of using agricultural residue as adsorbent precursor. The present study evaluates the adsorptive capacity of pineapple crown biochar in the removal of Cu²⁺ in aqueous solution through kinetic, equilibrium and thermodynamic studies of the adsorptive process. Kinetic evolution was rapid in the first minutes, reaching equilibrium around 180 minutes. The pseudo-second order model was the best fit to the obtained data. Langmuir's model better represented the experimental data. The maximum adsorptive capacity was $0.95 \pm 0.30 \text{ mmol}\cdot\text{g}^{-1}$. Thermodynamic study indicated physisorption process. The results demonstrated the potential of pineapple crown biochar for the adsorption of aqueous solutions Cu²⁺.

Keywords: Agro-industrial waste; Biochar; Copper.

1. Introduction

Industrial waste, without proper treatment, when disposed of in water bodies can cause environmental contamination and disease in living beings [1]. Among the pollutants frequently present in industrial effluents are heavy metals, such as copper, a substance listed by the Agency for toxic substances and disease registry (ATSDR) amongst the 785 most dangerous in the world [2].

In Brazil, the Resolution of the Conselho Nacional do Meio Ambiente (CONAMA) N° 430/2011 establishes the maximum content of copper (Cu²⁺) ions in effluents to be discharged into water bodies of $1.0 \text{ mg}\cdot\text{L}^{-1}$ [3].

The removal of this metal in effluents can be accomplished by the following methods: chemical precipitation, ultrafiltration, ion exchange, electrochemical treatment and adsorption [4].

Among these, adsorption is considered efficient in removing metals from effluents. It stands out for its simplicity of design, low initial investment, high efficiency for low concentration metal removal. ($\approx 100 \text{ mg}\cdot\text{L}^{-1}$), and the possibility of using residues as a precursor to obtain the adsorbent, making the

process even more attractive from an environmental point of view [5].

Among the residues that can be used as precursors to obtain adsorbents, agroindustrial ones stand out for their high carbon content [6]. Brazil is one of the largest pineapple producers in the world with a residue generation (crown, stems and cylinder) of 65% from the total fruit. The pineapple crown is considered as waste by the juice pulp industries and can be used as a precursor material [7].

Given the above the objective of this work was to prepare biochar from the pineapple crown (BCA) for removal of Cu²⁺ in aqueous solution. The kinetic and equilibrium studies were performed, with an adjustment of the models in their nonlinearized forms, and the thermodynamic survey.

2. Metodology

The pineapple crown (CA) was washed, dried at 105°C in an oven (Splabor) and ground in a knife mill. Subsequently, the material was carbonized in a muffle furnace (Chimis) using a heating ramp from $10^\circ\text{C}\cdot\text{min}^{-1}$ to 100°C (30 min), then to 200°C (1 h) and finally to 350°C (1 h). The prepared adsorbent

was called biochar from the pineapple crown (BCA) and classified in 0.090 mm particle size.

The Cu^{2+} ions concentration was quantified by Flame Atomic Absorption Spectrophotometry (Varian, SpectraAA 220 FS). An analytical curve with a linear working range of 1 to 280 $\text{mg}\cdot\text{L}^{-1}$ (0.016 to 4.4 $\text{mmol}\cdot\text{L}^{-1}$) was built at 222.6 nm wavelength, limit of detection of 0.4 $\text{mg}\cdot\text{L}^{-1}$ (0.007 $\text{mmol}\cdot\text{L}^{-1}$), limit of quantification 1.0 $\text{mg}\cdot\text{L}^{-1}$ (0.016 $\text{mmol}\cdot\text{L}^{-1}$), correlation coefficient of 0.99 and coefficient of variance of 4.27%. The adsorptive capacity (q_e) was calculated.

The adsorptive process was carried out in finite bath at $25.0 \pm 2.0^\circ\text{C}$, using 125 mL Erlenmeyer flasks that were stirred in a controlled manner (KS 130 control, IKA).

Kinetic, equilibrium and thermodynamic studies were performed under the experimental conditions determined at the preliminary test (0.1 g of adsorbent in contact with 50 mL of solution, pH 4.0 and 200 rpm).

2.1. Kinetic study of the adsorptive process

The kinetic study was performed using 0.1 g of the adsorbent in contact with Cu^{2+} solutions at concentrations of 0.05, 0.20, 0.50, 1.00 and 1.50 $\text{mmol}\cdot\text{L}^{-1}$, in the time interval from 0 to 300 min. The pseudo-first order (PFO) (Equation 1) and pseudo-second order (PSO) (Equation 2) kinetic models were fitted to the experimental data:

$$\frac{dq_t}{dt} = k_1(q_e - q_t) \quad (1)$$

$$\frac{dq_t}{dt} = k_2(q_e - q_t)^2 \quad (2)$$

in which: k_1 , the pseudo-first order adsorption constant (min^{-1}); k_2 is the pseudo-second order adsorption rate constant ($\text{g}\cdot\text{mmol}^{-1}\cdot\text{min}^{-1}$); q_e and q_t are the adsorptive capacity at equilibrium and time ($\text{mmol}\cdot\text{g}^{-1}$) respectively, and t is the time (minutes).

2.2. Adsorption equilibrium study

For the construction of the adsorption isotherm, the data obtained from the equilibrium kinetic study were used. The isotherm models used were Langmuir (Equation 3) and Freundlich (Equation 4).

$$q_e = \frac{q_{max} K_L C_e}{1 + K_L C_e} \quad (4)$$

$$q_e = K_F (C_e)^{1/n} \quad (5)$$

in which: q_{max} is the maximum adsorptive capacity ($\text{mmol}\cdot\text{g}^{-1}$); K_L , is the Langmuir isotherm constant, which represents the affinity between adsorbent and adsorbate ($\text{L}\cdot\text{mmol}^{-1}$); C_e , is the adsorbate concentration at equilibrium ($\text{mmol}\cdot\text{L}^{-1}$); K_F is the Freundlich constant indicating the adsorption capacity of the adsorbent ($\text{L}^{1/n}\cdot\text{g}^{-1}\cdot\text{mmol}^{1-1/n}$); and n indicates the efficiency of the adsorption process.

2.3. Thermodynamic Study

The thermodynamic study was performed at the temperatures of 303, 318 and 333 K, in the concentrations 0.2; 0.5; 1.1; 1.5; 2.0; 2.6; 3.0 and 4.7 $\text{mmol}\cdot\text{L}^{-1}$ of the Cu^{2+} solution. The thermodynamic parameters enthalpy (ΔH°), entropy (ΔS°) and adsorption heat (Q) were calculated.

3. Results and Discussion

3.1. Kinetic study in the adsorptive process

The kinetic study is one of the main parameters analyzed in the adsorptive process. Since, predicting the rate of removal of pollutants, establishing dependence over time and reveals the controlling mechanism of the adsorptive process [8]. The kinetic evolution curves of Cu^{2+} in contact with the BCA are present in Figure 1.

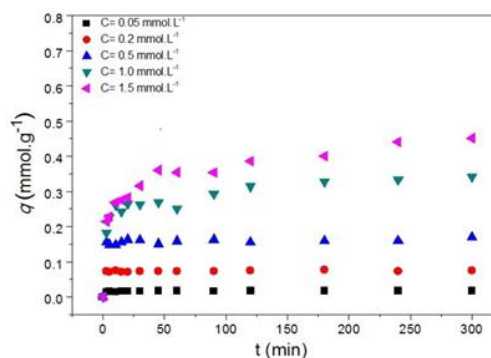


Fig. 1. Kinetic evolution of Cu^{2+} using the BCA. Conditions: 0.1 g in 50 mL of solution, $C_0 = 0.05 - 1.50 \text{ mmol}\cdot\text{L}^{-1}$; pH= 4.0 e 200 rpm.

It can be seen in Figure 1 that at the lowest concentrations (0.05 e 0.20 $\text{mmol}\cdot\text{L}^{-1}$) adsorption was rapid, possibly due to the number of active sites being greater than the number of ions present in the solution. At the highest concentrations, adsorption

was rapid in the early times, reaching equilibrium at 120 minutes.

The parameters of the PFO and PSO models were used to describe the Cu^{2+} ion adsorption kinetics and are presented in Table 1.

Table 1. Kinetic parameters for PFO and PSO models for Cu^{2+} ion adsorption by BC.

PFO					
C_0	$q_{e(\text{exp})}$	$q_{e(\text{calc})}$	k	SR ²	R ²
0.05	0.02	0.02	0.70	0.09	0.96
0.2	0.07	0.07	1.30	0.26	0.99
0.5	0.16	0.20	1.34	4.73	0.98
1.0	0.33	0.29	0.30	120.7	0.86
1.5	0.43	0.37	0.15	314.7	0.81
PSO					
0.05	0.02	0.02	0.90	0.06	0.98
0.2	0.07	0.07	1.40	0.22	0.99
0.5	0.16	0.16	0.34	3.91	0.98
1.0	0.33	0.31	0.014	71.44	0.92
1.5	0.43	0.40	0.005	140.2	0.91

According to Table 1, the values of $q_{e(\text{exp})}$ and $q_{e(\text{calc})}$ approximate for all concentrations in both models. The linear regression coefficients (R²) ranged from 0.81 to 0.99 for the PFO model and 0.91 to 0.99 for the PSO model. The PSO model presented a lower SR² variance, indicating that this model better represented the Cu^{2+} ion adsorption, expressing that the adsorption rate is not proportional to the solute concentration in agreement with Boundati et al. [9].

The PSO model also better represented the Cu^{2+} adsorption using maize silk reported by Petrović et al. [10].

3.2. Adsorption equilibrium study

The adsorption isotherms and nonlinear adjustments of the Langmuir and Freundlich models are presented in Figure 2 for the kinetic data corresponding to the 120 minutes time test when the system reaches equilibrium.

According to Figure 2, both models represent the interaction of adsorbent with Cu^{2+} ion. This can be verified through the parameters of the models (Table 2).

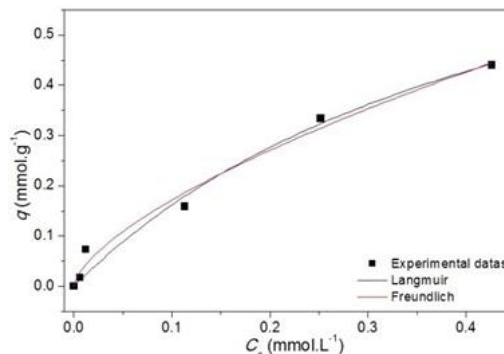


Fig. 2. Cu^{2+} adsorption isotherm using BCA. Conditions: 0.1 g in 50 mL of solution, $C_0 = 0.2$ to $4.7 \text{ mmol}\cdot\text{L}^{-1}$, pH= 4.0, 120 min. and 200 rpm.

Table 2. Parameters calculated for the equilibrium isotherm models.

Model	Parameters	Values
Langmuir	$q_{e(\text{calc})}$ ($\text{mmol}\cdot\text{g}^{-1}$)	0.95 ± 0.3
	K_L ($\text{L}\cdot\text{mmol}^{-1}$)	2 ± 1
	SR ²	0.003
	R ²	0.98
Freundlich	K_F ($\text{L}^{1/n}\cdot\text{g}^{-1}\cdot\text{mmol}^{1-1/n}$)	0.78 ± 0.08
	n	1.5 ± 0.1
	SR ²	0.002
	R ²	0.98

According to Table 2, it can be seen that the values of the correlation coefficients (R²) and the residuals left by the models (SR²) are similar indicating that the studied models describe the evaluated adsorptive process. This behavior can be attributed to the fact that the concentration of adsorbate was not sufficient to occupy the available sites.

The adsorptive capacities found in this work were compared with those presented in the literature (Table 3). In order to compare the values obtained in this work the maximum adsorptive capacities were converted to $\text{mmol}\cdot\text{g}^{-1}$.

Table 3. Comparison of the results obtained for Cu^{2+} ions by BCA with the literature.

Precursor	C_0 ($\text{mmol}\cdot\text{L}^{-1}$)	t (min)	q_{max} ($\text{mmol}\cdot\text{g}^{-1}$)	Authors
Corn silk	3.78	120	0.23	[8]
Peat moss	6.29	240	0.40	[10]
Pomegranate peel	0.79	120	0.32	[11]
BCA	1.49	120	0.73	This study

According to Table 3, the maximum adsorptive capacity (q_{\max}) of the BCA was higher than those obtained in the literature for similar equilibrium time. Comparing with the works of Petrović et al. [10] and Lee et al. [11], this work even with lower C_0 , obtained better adsorptive results.

3.2. Thermodynamic study

Adsorption isotherms at temperatures 303, 318 and 333 K are shown in Figure 3.

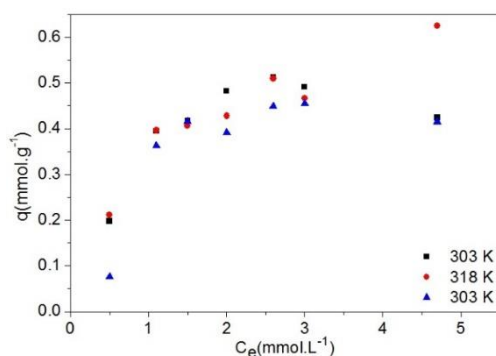


Fig. 3. Adsorption isotherms for Cu^{2+} by BCA at the temperatures of 303K, 318K and 303K.

From the Langmuir model fit to the experimental data of the three temperatures, the values of the adsorption equilibrium constants were obtained. From the slope of the $\ln(KL)$ versus T - plot it was possible to obtain the adsorption heat (Q) equals a $20.9 \text{ kJ}\cdot\text{mol}^{-1}$, (enthalpy) ΔH° equals to $14.20 \text{ kJ}\cdot\text{mol}^{-1}$ and entropy (ΔS°) equals to $0.05 \text{ kJ}\cdot\text{kmol}^{-1}$. The values obtained through the linear adjustments indicate that the process has a physical nature and there is the possibility of structural changes in the adsorbent/adsorbate ratio as according to Fito, Tefera and Hulle [12] and Piccin et al [13].

Acknowledgements

The authors would like to thank the Conselho Nacional de Desenvolvimento Científico e Tecnológico – Brazil (CNPq) and FADE/UFPE.

References

1] Asharaf A., Dutta J., Farooq A., Rafatullah M., Pal K., Kyzas G.Z. Chitosan-based materials for heavy metal adsorption: Recent advancements, challenges and limitations. *Journal of Molecular Structure*, 2024, 1309, 138225.

[2] Agency for toxic substances and disease registry (ATSDR), 2015. <https://www.atsdr.cdc.gov/spl/resources/atsdr_2015_spl_detailed_data_table.pdf>. Accessed 01 July 2024.

[3] BRASIL. Ministério do Meio Ambiente. Resolução nº 430, de 13 de maio de 2011. Conselho Nacional do Meio Ambiente (CONAMA), Brasília, DF, 2011.

[4] Sun J., He X., Le Y., Al-Tohamy R., Ali S.S. Potential applications of extremophilic bacteria in the bioremediation of extreme environments contaminated with heavy metals. *Journal of Environmental Management*, 2024, 352, 120081.

[5] Thotagamuge R., Kooh M.R.R., Mahadi A.H., Lim C.M., Abu M., Jan A. Hanipah A.H.A., Khiong Y.Y., Shofry A. Copper modified activated bamboo charcoal to enhance adsorption of heavy metals from industrial wastewater. *Environmental Nanotechnology, Monitoring & Management*, 2021, 16, 100562.

[6] Nascimento R.F., Sousa Neto V.O., Melo D.G., Sousa F.W., Cavalvante R.M. Uso de bioadsorvente lignocelulósicos na remoção de poluentes de efluentes aquosos. *Imprensa Universitária UFC*, 2014, 278p.

[7] Nunes JS, Lins ADF, Gomes JP, Silva WP, Silva FB. Influência da temperatura de secagem nas propriedades físico-química de resíduos de abacaxi. *Revista Agropecuária Técnica*, 2017, 1, 41-46.

[8] Guo X, Wang J. A general kinetic model for adsorption: Theoretical analysis and modeling. *J. of Mol. Liq.* 2019, 288, 111100. <https://doi.org/10.1016/j.molliq.2019.111100>

[9] Boundati YE, Ziat K, Naji A, Saidi M. Generalized fractal-like adsorption kinetic models: Application to adsorption of copper on Argan nut shell. *J. Mol. Liq.* 2019, 276, 15-26.

[10] Petrović M, Šoštarić T, Stojanović M, Petrović J, Mihajlović M, Čosović A, Stanković S. Mechanism of adsorption of Cu^{2+} and Zn^{2+} on the corn silk (*Zea mays* L.). *Ecol Eng* 2017; 99: 83–90.

[11] Lee S, Park JH, Ahn Y, Chung JW. Comparison of Heavy Metal Adsorption by Peat Moss and Peat Moss-Derived Biochar Produced Under Different Carbonization Conditions. *Water Air Soil Pollut*, 2015, 226, 9-19.

[12] Fito J, Tefera N, Van Hulle SWH. Adsorption of distillery spent wash on activated bagasse fly ash: Kinetics and thermodynamics. *J. Environ. Chem. Eng.*, 2017, 5, 5381–5388.

[13] Piccin JS, Cadaval JrTRS, Pinto LADE, Dotto GL. Adsorption Isotherms in Liquid Phase: Experimental, Modeling, and Interpretations. *Adsorption. Process. Water Treat. Purif.*, 2017, 19-51.